



SCUOLA INTERNAZIONALE SUPERIORE DI STUDI AVANZATI

SISSA Digital Library

How localized bosons manage to become superfluid

Original

How localized bosons manage to become superfluid / Dell'Anna, L; Fabrizio, Michele. - In: JOURNAL OF STATISTICAL MECHANICS: THEORY AND EXPERIMENT. - ISSN 1742-5468. - 2011:8(2011), pp. 1-20. [10.1088/1742-5468/2011/08/P08004]

Availability:

This version is available at: 20.500.11767/14225 since: 2023-08-08T11:37:29Z

Publisher:

Published

DOI:10.1088/1742-5468/2011/08/P08004

Terms of use:

Testo definito dall'ateneo relativo alle clausole di concessione d'uso

Publisher copyright

IOP- Institute of Physics

This version is available for education and non-commercial purposes.

note finali coverpage

(Article begins on next page)

How localized bosons manage to become superfluid

Luca Dell'Anna¹ and Michele Fabrizio^{2,3}

¹ *Dipartimento di Fisica “G. Galilei”, Università di Padova, 35131, Italy*

² *International School for Advanced Studies, SISSA, 34136 Trieste, Italy*

³ *International Centre for Theoretical Physics, ICTP, 34151 Trieste, Italy*

(Dated: November 7, 2018)

Abstract

We show that the many-body wavefunction built as a permanent of localized non-orthogonal single-particle states can describe bosonic superfluidity. The criterium for the transition is expressed in terms of the properties of the matrix of the overlaps between the single-particle wavefunctions. We apply this result to study the superfluid-to-Bose glass transition in a disordered Bose-Hubbard model through a very simple variational wavefunction. We finally consider a further quantity, the bipartite entanglement entropy, which also provides a good estimator for the superfluid-to-Bose glass transition.

PACS numbers: 05.30.Jp, 03.67.Mn, 64.70.Tg

I. INTRODUCTION

The study of the interplay between disorder and interaction has recently received novel impulse by the experimental realizations of correlated and disordered systems through optical lattices.[1, 2] Particular interest has been devoted to trapped bosonic atoms in the presence of on-site disorder, which can be simulated experimentally using speckles or superimposing incommensurate laser beams.[3–5] The great opportunity offered by this kind of experiments is that not only disorder can be easily tuned but also the interaction among the atoms, this latter by means of the Feshbach’s resonance technique.[6] These experiments have motivated a renewed theoretical activity on the phase diagram of the disordered Bose-Hubbard model [7–15], an old[16–21] but still debated issue. This model is supposed to exhibit three different phases. Besides the Mott-insulating phase, occurring when interaction is strong and the particle density is commensurate, and the superfluid phase, stable for weak interaction, in the presence of disorder an additional phase has been predicted to occur,[18] the so-called Bose glass. Such a disorder driven phase is supposed to be insulating but, unlike the Mott insulator, compressible. In the absence of interaction, the Bose glass is simply the state obtained by condensing all bosons in the lowest energy eigenstate of the single-particle disordered Schrödinger equation, which is supposed to lie in the Lifshits’s tail of localized wavefunctions. This picture is however unstable to whatever weak interaction, since a macroscopic occupancy of a finite region in real space would be energetically unbearable. In fact, a more realistic view of a Bose glass is that of disconnected superfluid droplets, where coherent inter-droplet tunneling is inhibited by the Anderson localization phenomenon, hence the insulating behavior, yet transferring electrons between different droplets is costless, hence the finite compressibility.

In this paper, we investigate the superfluid-to-Bose glass transition by means of a very simple variational wavefunction. It consists of a permanent of non-orthogonal single-particle wavefunctions that are determined in a variational manner. Although the approach is not as rigorous as e.g. quantum Monte Carlo,[8, 10, 13, 15] nevertheless it provides a very transparent description of the transition and of the same Bose glass. Indeed, all coherence properties of the wavefunction are hidden in the single-particle wavefunctions that build the permanent. In particular, since these wavefunctions need not to be orthogonal, it is their overlap matrix that seems to play an important role. Actually one can derive an approximate

criterion for the permanent to have macroscopic condensation at zero momentum, hence superfluidity, which involves just the overlap matrix. We find that this criterium agrees well with the more rigorous one based on the superfluid stiffness.

Finally, in the last part of the paper we study the single site von Neumann entropy, which could also be used to identify the superfluid-to-Bose glass transition. The quantum entanglement applied to many body systems has attracted lot of theoretical interest in recent years (see for instance Refs. [22–25] and references therein). So far, however, the entanglement witnesses have never been used in the context of disordered Hubbard model. We show that, within our variational approach, the Bose glass seems to be characterized by a finite probability of the single-site von Neumann entropy to have zero value. In other words, as disorder increases, the entropy distribution gets broaden and broaden until the probability to have zero entropy becomes finite, which we identify as the onset of Bose glassiness. This criterium is qualitatively good as far as we deal with small system size since the zero entropy is the signature of vanishing charge fluctuations in some regions of the sample which becomes then easily disconnected. A more quantitative analysis for large systems would involve the study of the entropy distribution and the appearance of the bimodal profile in agreement with the droplet scenario. Our conjecture is that the weights and the positions of the two modes at the transition should be related to the percolation threshold.

The paper is organized as follows. In Sec. II we present a criterium for the onset of superfluidity that is based on the matrix of the overlaps between the single particle wavefunctions that built the variational many-body wavefunction. In Sec. III we introduce the disordered Bose-Hubbard model and in Sec. IV we describe the variational many-body wavefunction that we study. Sec. V is devoted to studying the bipartite entanglement entropy as another tool to identify the superfluid-to-Bose glass transition. Final conclusions are summarized in Sec. VI.

II. OVERLAP MATRIX CRITERIUM

Let us imagine a Hartree-Fock-like variational approach to the problem of disordered and interacting bosons that amounts to search for the permanent that minimizes the total energy. Unlike conventional Hartree-Fock theory for fermions, such an approximation for bosons does not lead to significant simplifications with respect to exact numerical simulations

because permanents are extremely difficult to handle with. Nonetheless, let us assume we have successfully performed the calculation and found the optimal permanent for N particles, which can be written as

$$|\Psi\rangle = \prod_{\alpha=1}^N \left(\sum_i \psi_{\alpha i} b_i^\dagger \right) |0\rangle, \quad (1)$$

in terms of a set of single particle wavefunctions ψ_α , with amplitude $\psi_{\alpha i}$ at site i . In (1) b_i^\dagger creates a boson at site i . Unlike Slater determinants, the wavefunctions that built a permanent need not to be orthogonal one to each other, so we expect the overlap matrix Ω to have non-zero off-diagonal elements $\Omega_{\alpha\beta} = \sum_i \psi_{\alpha i} \psi_{\beta i}^*$. For instance, if all bosons condense into a single state, then all ψ_α are equal and $\Omega_{\alpha\beta} = 1$, $\forall \alpha, \beta \in [1, N]$. In the generic case where ψ_α are distinct, we may wonder whether wavefunction (1) describes a superfluid. In what follows we derive a simple criterium that is based on the properties of the overlap matrix.

One can verify that the norm of (1) can be written as an integral over classical variables as[18]

$$\langle \Psi | \Psi \rangle = \int \prod_{\alpha} \frac{d\xi_{\alpha} d\xi_{\alpha}^*}{\pi} e^{-\mathcal{S}(\xi, \xi^\dagger)} \quad (2)$$

with the following action (see Appendix A)

$$\mathcal{S}(\xi, \xi^\dagger) = \xi^\dagger (\Omega - \mathbb{1})^{-1} \xi - \sum_{\alpha} \ln \left(1 + |\xi_{\alpha}|^2 \right). \quad (3)$$

We assume that the main contribution to the integral comes from the saddle point, i.e. the solution of

$$\xi_{\alpha} = \sum_{\beta} (\Omega_{\alpha\beta} - \delta_{\alpha\beta}) \frac{1}{1 + |\xi_{\beta}|^2} \xi_{\beta}. \quad (4)$$

The above equation implies that finite values of ξ_{α} appear in groups, or equivalently that Ω is a block matrix. In the presence of disorder this is suggestive of the existence of clusters occupied by bosons whose wavefunctions mutually overlap. Because of interaction, a cluster can not accomodate all particles unless it covers all the system, which would correspond also to superfluidity. If we linearize (4), we find that the condition for the apperance of a cluster reads

$$\xi_{\alpha} = \sum_{\beta} (\Omega_{\alpha\beta} - \delta_{\alpha\beta}) \xi_{\beta}, \quad (5)$$

which corresponds to a block of Ω that acquires an eigenvalue greater than two. As we mentioned, this is still not the condition for superfluidity. The latter rather implies that a

block in Ω should grow, or several blocks should merge, i.e. start to overlap, till a percolating cluster emerges. This condition is likely to be equivalent to an eigevalue of Ω that grows with the number of bosons N . We finally mention that the saddle point approximation that we used is rigrouslly valid only if blocks are big enough.

A. Density matrix and overlap condition

A better and more transparent criterium to detect a long range order is to resort to the definition of the density matrix,

$$C_{ij} = \langle \Psi | b_i^\dagger b_j | \Psi \rangle. \quad (6)$$

Off-diagonal long-range order implies that C_{ij} is finite for $|i - j| \rightarrow \infty$. Within the path integral formulation, using Eqs. (A2), (A6), one can verify that C_{ij} can be written as

$$C_{ij} = \sum_{\alpha\beta} \psi_{i\alpha}^\dagger \langle \xi_\alpha \xi_\beta^\dagger \rangle \psi_{\beta j} \quad (7)$$

where $\langle \dots \rangle$ is now the average weighted by $e^{-\mathcal{S}}$, with the action \mathcal{S} given by Eq. (3). If the saddle point of the action is characterized by finite ξ_α , one could be tempted to set

$$\langle \xi_\alpha \xi_\beta^\dagger \rangle \simeq \langle \xi_\alpha \rangle \langle \xi_\beta^\dagger \rangle. \quad (8)$$

This is not fully correct. Indeed, if Ω is a block matrix, within each block only the relative phases of the ξ_α are fixed, while an overall phase is still free and has to be integrated out. This implies that (8) is correct only if α and β are within the same block, otherwise the relative phase between the two blocks will suppress the average. This suggests that off-diagonal long-range order sets up only if a single block percolates. More rigorously, we define

$$\xi_i = \sum_{\alpha} \psi_{i\alpha}^\dagger \xi_\alpha, \quad (9)$$

through which the density matrix reads

$$C_{ij} = \langle \xi_i \xi_j^\dagger \rangle. \quad (10)$$

The saddle point equation in terms of ξ_i is

$$2 \xi_i = \sum_j O_{ij} \xi_j, \quad (11)$$

where

$$O_{ij} = \sum_{\alpha} \psi_{\alpha i}^* \psi_{\alpha j}, \quad (12)$$

is the density matrix of the wavefunctions. An extreme superfluid solution identified by $\xi_i = \xi$, $\forall i$ could be stabilized if

$$\mathcal{F} \equiv \frac{1}{N_s} \sum_{ij} O_{ij} \geq 2, \quad (13)$$

where N_s is the number of sites.

B. An example: the bosonic crystal

As a simple application of the previous results we shall now investigate the possibility that a permanent that describes at the ‘‘Hartree-Fock’’ level a Bose-Wigner crystal, could be also superfluid, actually a supersolid. Let us consider a commensurate density $N/N_s < 1$ of interacting bosons on a lattice with N_s sites in the absence of disorder. If the repulsion is sufficiently strong and long ranged, we may imagine that the best variational permanent wavefunction describes a bosonic superlattice with Bravais vectors

$$\mathbf{R} = a(m_1, m_2, \dots, m_d), \quad (14)$$

where a is the superlattice parameter. We write the Wannier single-particle wavefunctions that correspond to the Bose-Wigner crystal as

$$\psi_{\mathbf{R}}(\mathbf{R}_i) = \sqrt{\frac{1}{N_s}} \sum_{\mathbf{k}} u_{\mathbf{k}} e^{i\mathbf{k}(\mathbf{R}-\mathbf{R}_i)}, \quad (15)$$

where \mathbf{k} runs within the Brillouin zone of the original lattice, \mathbf{R}_i spans all lattice sites while \mathbf{R} only the superlattice ones. The permanent is therefore

$$|\Psi\rangle = \prod_{\mathbf{R}} \left(\sum_i \psi_{\mathbf{R}}(\mathbf{R}_i) b_i^\dagger \right) |0\rangle. \quad (16)$$

In this case the overlap matrix is

$$\Omega_{\mathbf{R}\mathbf{R}'} = \frac{1}{N_s} \sum_{\mathbf{k}} |u_{\mathbf{k}}|^2 e^{i\mathbf{k}(\mathbf{R}-\mathbf{R}')}. \quad (17)$$

We assume for simplicity that the wavefunction is gaussian,

$$u_{\mathbf{k}} = \frac{1}{v} \left(\frac{\ell}{\sqrt{\pi}} \right)^d e^{-\ell^2 |\mathbf{k}|^2 / 4\pi^2}, \quad (18)$$

where v is the volume of unit cell and ℓ the localization length, so that the overlap matrix has the simple expression

$$\Omega_{\mathbf{R}\mathbf{R}'} = e^{-\pi^2 \frac{|\mathbf{R}-\mathbf{R}'|^2}{\ell^2}}, \quad (19)$$

and depends only on the distance, $\Omega_{\mathbf{R}\mathbf{R}'} = \Omega_{\mathbf{R}-\mathbf{R}'}$. From the saddle point equation we find that the condition to have superfluidity is simply

$$\sum_{\mathbf{R}} \Omega_{\mathbf{R}} = \sum_{\mathbf{R}} e^{-\pi^2 \frac{|\mathbf{R}|^2}{\ell^2}} \geq 2. \quad (20)$$

By means of the Jacobi theta function $\theta_3(0|x) = \sum_{m=-\infty}^{\infty} x^{m^2}$, Eq. (20) means

$$\theta_3\left(0|e^{-\pi^2 a^2/\ell^2}\right) \geq \sqrt[4]{2}. \quad (21)$$

The condition Eq. (21) fixes the critical overlap between the Wannier functions, parametrized by the ratio ℓ/a , above which bosons condense at zero momentum, i.e. the many-body wavefunction describes a supersolid.

In the next section we shall consider the Bose-Hubbard model in the presence of disorder which causes now the localization of the single-particle wavefunctions. We are going to see that, also in that case, in spite of the Anderson localized nature of the single-particle states obtained variationally, the many-body wavefunction can be superfluid.

III. THE MODEL

We consider a system of interacting bosons on a disordered 2-dimensional lattice with $N_s = L^2$ sites, described by the following Bose-Hubbard hamiltonian

$$H = -\frac{t}{2} \sum_{\langle ij \rangle} \left(b_i^\dagger b_j + H.c. \right) + \sum_i \epsilon_i n_i + \frac{U}{2} \sum_i n_i (n_i - 1), \quad (22)$$

where b_i^\dagger (b_i) creates (annihilates) a boson at site \mathbf{R}_i , $\langle ij \rangle$ denotes the sum over all pairs of neighboring sites, $n_i = b_i^\dagger b_i$ is the boson local density, and, finally, ϵ_i are random on-site energies uniformly distributed between $-\Delta$ and Δ .

Since the seminal works of Giamarchi and Schulz[16, 17] and Fisher *et al.*[18], the Hamiltonian (22) has been studied with a variety of techniques, mainly in one and two dimensions. More recently, highly sophisticated numerical simulations[7, 8, 10, 13–15, 20, 21] have been performed to uncover the full phase diagram and settle up some debated issues, like the

possibility of a direct superfluid-Mott insulator transition. The results we are going to present are by no means comparable in accuracy with the aforementioned numerical simulations. Our main purpose is not to compete with those simulations, but just to provide an interpretation of the phase diagram in terms of a simple Hartree-Fock-like single-particle picture.

IV. THE METHOD

The simplest way to deal with interacting electrons is the Hartree-Fock approximation, which amounts to search for the best wavefunction within the subspace of Slater determinants. This approximation reduces the complicated many-body problem to a single-particle one with an effective potential generated by all other particles. Even more realistic approaches, like the Density-Functional theory in the Local Density approximation, eventually reduces to the self-consistent solution of a single-particle Schrödinger equation. The great advantage is that a single-particle description is very intuitive and, although it could be too naïve in many cases, at least it is a simple starting point for more complicated approaches.

The obvious generalization of the Hartree-Fock approximation to interacting bosons would be searching for the best wavefunction within the subspace of permanents, the bosonic analogues of Slater determinants. However, as we already mentioned, unlike Slater determinants, permanents are well defined even if the single-particle wavefunctions that are used are not orthogonal to each other. Therefore the optimization procedure is not reduced to solving a single eigenvalue problem, which would produce a set of orthogonal wavefunctions, but becomes rather complicated, practically unfeasible, hence further approximations are required.[26]

Our simplified approach consists in adding one boson at a time with a wavefunction that is the ground state of a non-interacting Hamiltonian with a potential determined by the already added bosons. Specifically, we consider the not normalized N boson wavefunction

$$|\Psi_N\rangle = \prod_{\alpha=1}^N \left(\sum_j \chi_{\alpha j} b_j^\dagger \right) |0\rangle \quad (23)$$

where $\chi_{\alpha j}$, $j = 1, \dots, N_s$ are generically non-orthogonal single-particle wavefunctions. The first wavefunction χ_{1j} is the ground state of (22) with $U = 0$ (no bosons are present). The

$(M + 1)$ -th wavefunction is instead the ground state of

$$H_{app} = -\frac{t}{2} \sum_{ij} b_i^\dagger b_j + \sum_i \left(\epsilon_i + U \langle n_i \rangle \right) n_i, \quad (24)$$

where

$$\langle n_i \rangle = \frac{\langle \Psi_M | b_i^\dagger b_i | \Psi_M \rangle}{\langle \Psi_M | \Psi_M \rangle}, \quad (25)$$

is the average density of the previously added M bosons. We define an $M \times M$ matrix

$$\Omega_{\alpha\beta} = \sum_{i=1}^{N_s} \chi_{\alpha i} \chi_{\beta i}^* \quad (26)$$

$\alpha, \beta = 1, \dots, M$, and, for each couple of lattice sites (i, j) , the $(M + 1) \times (M + 1)$ matrices

$$D_{ij} = \begin{pmatrix} \Omega & \hat{\chi}_i \\ \hat{\chi}_j^\dagger & \delta_{ij} \end{pmatrix}$$

where $\hat{\chi}_i = (\chi_{1i}, \dots, \chi_{Mi})^t$. It follows that the mean local density that is required for adding the next $(M + 1)$ -th boson, namely Eq.(25), can be written as follows

$$\langle n_i \rangle = \frac{\text{Per}(D_{ii})}{\text{Per}(\Omega)} - 1 \quad (27)$$

where $\text{Per}(X)$ is the permanent of X . At each iteration, one can also calculate the inter-site density matrix, since

$$C_{ij} \equiv \frac{\langle \Psi | b_i^\dagger b_j | \Psi \rangle}{\langle \Psi | \Psi \rangle} = \frac{\text{Per}(D_{ji})}{\text{Per}(\Omega)} - \delta_{ij}, \quad (28)$$

hence investigate the eventual offset of long-range order. This procedure is iterated until the desired number N of bosons is reached. We note that the method can be easily extended to study excited states – it is sufficient to select at any iteration not the ground state but an excited one – hence at finite temperature, even though in what follows we just focus on the lowest energy states.

The superfluid properties of the model can be accessed by calculating the superfluid stiffness ρ_{sf} defined through

$$\rho_{sf} \simeq \frac{L^2}{N} \left. \frac{\partial^2 E_\theta}{\partial \theta^2} \right|_{\theta=0}, \quad (29)$$

where E_θ is the average value of the Hamiltonian (22) with twisted boundary conditions along a given direction \mathbf{x} , or, alternatively, with hopping parameter between neighboring sites $t_{ij} = t e^{i\theta \vec{r} \cdot \vec{x}}$, where $\vec{r} = (\mathbf{R}_i - \mathbf{R}_j)/L$. In terms of permanents we calculate

$$E_\theta = - \sum_{ij} \left(\frac{t_{ij}}{2} - \delta_{ij}(\epsilon_i - 2U) \right) C_{ij} + \frac{U}{2} \sum_i \left(\frac{\text{Per}(I_{iiii})}{\text{Per}(\Omega)} - 2 \right) \quad (30)$$

where C_{ij} is defined in Eq. (28) and $\text{Per}(I_{ijkl}) = \langle \Psi | b_i b_j b_k^\dagger b_l^\dagger | \Psi \rangle$ with

$$I_{ijkl} = \begin{pmatrix} \Omega & \hat{\chi}_i & \hat{\chi}_j \\ \hat{\chi}_k^\dagger & \delta_{ik} & \delta_{jk} \\ \hat{\chi}_l^\dagger & \delta_{il} & \delta_{jl} \end{pmatrix}. \quad (31)$$

Upon repeating this calculation for several disorder configurations, averaging over them and setting equal to zero the stiffness in the region of parameters where its variance is greater than its average (cutting, therefore, the values of ρ_{sf} statistically undetermined), we finally obtain the phase diagram of Fig.1, which is a contour-plot of the averaged superfluid stiffness ρ_{sf} of a 2-dimensional model with filling fraction $\nu = N/N_s = 1/4$. We note that in a finite system there cannot be a true gauge-symmetry breaking, hence the phase diagram Fig.1 is just an indication of what could happen in the thermodynamic limit. Nevertheless, the qualitative behavior that we find is physically sensible: ρ_{sf} decreases on increasing disorder and, at fixed disorder, first increases with U and then diminishes. In Fig. 1 and in the following figures the values of U and Δ are in units of t .

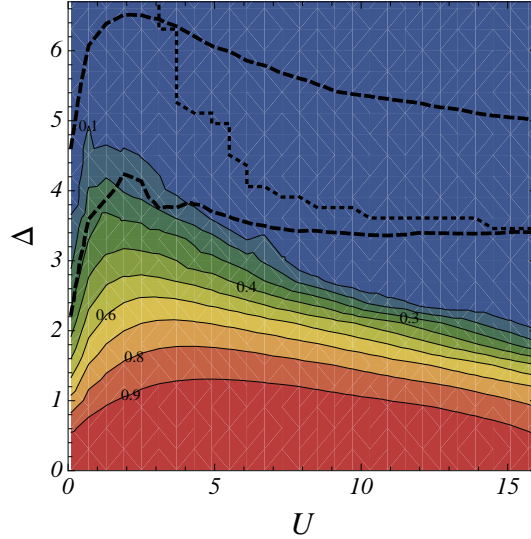


FIG. 1: (Color online) Contour-plot of the superfluid stiffness ρ_{sf} , Eq. (29), for a 6×6 square lattice at filling $\nu = 1/4$, averaging over 400 disorder configurations. The two thick dashed lines and the dotted line show the border of the superfluid phase, by looking at some indicators related to the overlap matrix, as discussed in Sec. IV A.

We previously mentioned that a realistic view of a Bose glass is that of disconnected droplets. A way to confirm this idea is plotting the average density as shown in Fig. 2,

where we used, instead of Eq. (25), $\langle n_i \rangle \simeq \sum_{\alpha}^N |\chi_{\alpha i}|^2$, which is a good approximation for local densities, in order to computationally reach larger system sizes. We find that, at large disorder, bosons are indeed concentrated into droplets whose magnitude increases on decreasing disorder until a percolating cluster appears, which must presumably signal the onset of superfluid.

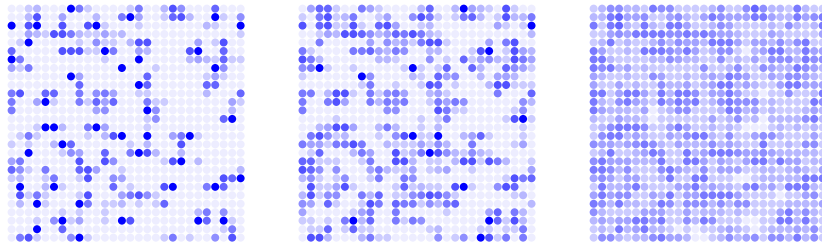


FIG. 2: (Color online) Contour plot of the particle density $\langle n_i \rangle$ on a 28×28 lattice with $N = 49$ bosons, i.e. filling $\nu = 1/16$, at $U = 10$ and for a single realization of disorder with $\Delta = 1, 2, 3$ from right to left (i.e. crossing the transition, see inset of Fig. 6). The darker the sites the higher is the density.

A. Comparison with the overlap matrix method

Let us compare the transition obtained by the superfluid stiffness with that given by the overlap matrix criterium. In our case, given the many-body wavefunction Eq. (23), the overlap matrix Ω is that defined in Eq. (26) with $\psi_{\alpha i} = \chi_{\alpha i}$. The action is given by Eq. (3) and the saddle point equation reads as in Eq. (5), which has non trivial solution if Ω has eigenvalue 2.

In Fig. 1 we plot a dotted line below which $(\Omega - 2\mathbb{1})$, or equivalently, $(O - 2\mathbb{1})$, has both positive and negative eigenvalues for any disorder configuration, implying that the saddle point equation has always non trivial solutions. Above that line, instead, for some disorder configurations all the eigenvalues of Ω are smaller than 2.

On the same figure, Fig. 1, we plot two thick dashed lines which correspond to $\overline{\mathcal{F}} = 2$ (the upper line), namely, when the value of \mathcal{F} as defined in Eq. (13), averaged over 400 disorder configurations, equals 2, and $\min(\mathcal{F}) = 2$ (lower line), namely, when the minimum value of \mathcal{F} among the disorder configurations equals 2. Below those lines the corresponding

quantities exceed the threshold value. Notice that a non trivial solution of the saddle point equation occurs also for large disorder and weak interaction (the dotted line keeps on growing decreasing U) while \mathcal{F} , which detects the long range order (dashed lines), follows correctly the stiffness behavior also for small interaction.

In summary, we find that the superfluid properties of the many-body wavefunction (23) can be related to the overlap matrix Ω between the single-particle wavefunctions $\chi_{\alpha i}$. This result also clarifies why, even though each wavefunction $\chi_{\alpha i}$ is the lowest energy solution of the Schrödinger equation of a particle in a disordered potential, hence would be always localized in two dimensions, and also in higher dimensions if, as presumably is the case, it lies in the Lifshitz tail, nevertheless the permanent built with them could still be superfluid.

A final comment. We optimized the wavefunction by explicitly evaluating permaments. This is in general very cumbersome, not much simpler than an exact numerical solution of the problem, which is the reason why our simulation size is small. However, we could adopt an oversimplified approach and evaluate the Hartree potential in Eq. (24) for the $(M+1)$ -th boson using

$$\langle n_i \rangle \simeq \sum_{\alpha=1}^M |\chi_{\alpha i}|^2, \quad (32)$$

as if the already present M bosons were distinguishable. This approximation simplifies a lot the procedure to determine the single-particle wavefunctions, which can be pushed to very large system sizes. These single-particle wavefunctions can then be used to construct the permanent, whose superfluid properties can be assessed by the overlap matrix criterium. Even though such a procedure is hardly justifiable from the variational point of view, it provides a phase diagram qualitatively correct. Using this approximation one can study the spectrum of the overlap matrix Ω for larger system, finding that, indeed, the transition is characterized by the fact that the greatest eigenvalue of Ω starts growing towards value N , the number of bosons, for Δ going to zero. From Fig. 3 one can see clearly, in fact, that a single eigenvalue of Ω (although quite noisy, it is a single level) separates from the others at $\Delta \approx 4$, approximately at the same value of disorder as that obtained for a smaller system size with $\langle n_i \rangle$ given by (27) (cfr. the transition line at $U = 10$ in Fig. 1). The other eigenvalues (see the inset of Fig. 3) accumulate around zero below the transition, and around one above it, at least for filling not greater than one, as in our case.

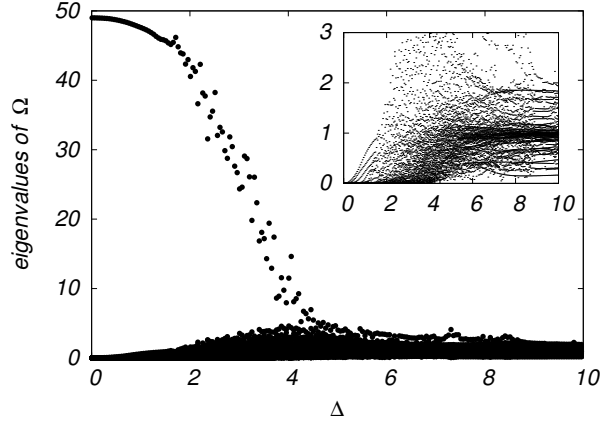


FIG. 3: Eigenvalues of Ω as functions of Δ , at a given configuration of disorder, for 49 bosons on a square lattice with 256 sites, namely always for filling $1/4$, at $U = 10$. The inset magnifies the lower part of the main plot.

V. SPATIAL ENTANGLEMENT ENTROPY

Another quantity which may be interesting to look at is the single site entanglement entropy. We define as $\rho_n(i)$ the probability to have n bosons at site i , which must trivially satisfy $\sum_{n=0}^N \rho_n(i) = 1$, where N is the total number of bosons. The single-site entropy S_i is thus defined through

$$S_i = - \sum_{n=0}^N \rho_n(i) \ln \rho_n(i). \quad (33)$$

In a disordered system it is also convenient to define its probability distribution through

$$P(S) = \langle \frac{1}{N_s} \sum_i \delta(S - S_i) \rangle_{disorder}, \quad (34)$$

which is obtained considering all sites and all disorder configurations. In spite of its simple definition, we are going to show that the single-site entanglement entropy, and especially its distribution probability, is a quite enlighting quantity in the presence of both disorder and interaction.

A. A limiting case

We start considering the case where all bosons condense into a single state, i.e. $\chi_{\alpha j} = \zeta_j$, $\forall \alpha$, with the normalization condition $\sum_{j=1}^{N_s} \zeta_j = 1$. In this case $\text{Per}(\Omega) = N!$ and the state

Eq. (23), including the normalization factor $1/\sqrt{\text{Per}(\Omega)}$ can be decomposed in the site Fock basis as

$$|\Psi\rangle = \frac{1}{\sqrt{N!}} \left(\sum_j \zeta_j b_j^\dagger \right)^N |0\rangle = \sum_{\{n\}} \frac{\sqrt{N!}}{\prod_i n_i!} \prod_{j=1}^{N_s} \zeta_j^{n_j} (b_j^\dagger)^{n_j} |0\rangle. \quad (35)$$

The sum runs over $\{n\} = (n_1, n_2, \dots, n_{N_s})$, the configurations of occupation numbers with the constraint $\sum_i n_i = N$. We calculate the reduced density matrix $\hat{\rho}^\ell$ by partitioning the sites in two blocks: $[1, \ell]$ and $[\ell, N_s]$, and tracing out the sites belonging to the second block:

$$\hat{\rho}^\ell = \sum_{n_{\ell+1}, \dots, n_{N_s}} \frac{1}{\prod_{i=\ell+1}^{N_s} n_i!} \langle 0 | \prod_{i=\ell+1}^{N_s} (b_i)^{n_i} |\Psi\rangle \langle \Psi | \prod_{i=\ell+1}^{N_s} (b_i^\dagger)^{n_i} |0\rangle. \quad (36)$$

This is a diagonal $\frac{(N+1)!}{\ell!(N+1-\ell)!} \times \frac{(N+1)!}{\ell!(N+1-\ell)!}$ matrix. For each diagonal element $\rho_{n_1, \dots, n_\ell}$, corresponding to the configuration of the occupation numbers $(n_1, n_2, \dots, n_\ell)$ of the ℓ sites that are not traced out, we obtain the following expression

$$\rho_{n_1, \dots, n_\ell} = \frac{N!}{(N - \sum_{i=1}^\ell n_i)! \prod_{i=1}^\ell n_i!} \left(1 - \sum_{i=1}^\ell |\zeta_i|^2 \right)^{(N - \sum_{i=1}^\ell n_i)} \prod_{i=1}^\ell |\zeta_i|^{2n_i}. \quad (37)$$

From now on we shall focus on the simplest partitioning, keeping only one site and tracing over all the others, i.e. $\ell = 1$. In this case we get a very simple binomial expression of the reduced density matrix $\rho_n \equiv \rho_n(1)$

$$\rho_n = \binom{N}{n} (1 - |\zeta_1|^2)^{(N-n)} |\zeta_1|^{2n}. \quad (38)$$

It is straightforward to check that $\sum_n \rho_n = 1$. The reduced density matrix is fully local; it depends only on the value of the wavefunction ζ on that site. We can now calculate the entanglement von Neumann entropy at site 1, S_1 , through (33). From Eqs. (38) and (33) we find that for any fixed value of $|\zeta_1| \in (0, 1)$ and for large N , the asymptotic value of S_1 is

$$S_1 \xrightarrow{N \gg 1} S_{loc} \equiv \frac{1}{2} \ln N + A, \quad (39)$$

with $A = \frac{1}{2} \{1 + \ln [2\pi |\zeta_1|^2 (1 - |\zeta_1|^2)]\}$. At the two extremes, $|\zeta_1| = 0, 1$, we have $S_1 = 0$.

Let us consider first the non-interacting case with disorder. All bosons condense into a localized wavefunction. Within the localization region $S_i \sim \ln N$, while outside $S_i = 0$. We conclude that the probability distribution (34) becomes peaked at the single value $S = 0$

in the thermodynamic limit, $N_s \rightarrow \infty$, where the localization region has zero measure with respect to the whole system.

On the contrary, without disorder and deep in the superfluid phase, small U , we expect that

$$|\zeta_1|^2 = \frac{1}{N_s} = \frac{\nu}{N} \quad (40)$$

where the filling fraction $\nu = N/N_s$. In this case, the single-site entropy in the thermodynamic limit is finite, site-independent and depends exclusively on the filling fraction ν :

$$S_1 \xrightarrow{N \rightarrow \infty} S_{SF} \equiv \nu(1 - \ln \nu) + e^{-\nu} \sum_{n=0}^{\infty} \frac{\nu^n}{n!} \ln n! \quad (41)$$

The sum Eq. (41) converges for any value of ν . As one can see from Fig. 4, the thermodynamic limit Eq. (41) is approached already with few bosons, for small ν . In the same figure we also draw the maximum entropy line, Eq. (39), which indeed lies above all curves.

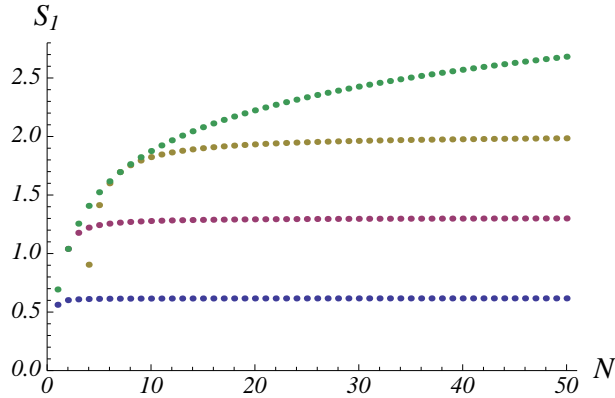


FIG. 4: (Color online) Single site entanglement entropies obtained by Eqs. (38), (33). Upper dot-line: the maximum entropy, reached when $|\zeta_1|^2 = 1/2$. Upper middle dot-line: entropy for the superfluid with $\nu = 7/2$ case, i.e. for $|\zeta_1|^2 = 7/(2N)$. Lower middle dot-line: entropy for the superfluid in the commensurate $\nu = 1$ case, i.e. for $|\zeta_1|^2 = 1/N$. Lower dot-line: the superfluid entropy for $|\zeta_1|^2 = 1/(4N)$, i.e. $\nu = 1/4$.

In conclusion, we expect that the probability distribution of the single-site entropy is peaked at a finite value deep in the superfluid phase while at value zero deep in the Bose-glass phase. The obvious question is what happens in between.

B. Single-site entropy across the superfluid-to-Bose glass transition

Let us now consider the state Eq. (23), including the normalization factor $1/\sqrt{\text{Per}(\Omega)}$, which in the Fock basis of sites reads

$$|\Psi\rangle = \frac{1}{\sqrt{\text{Per}(\Omega)}} \sum_{\{n\}} \sum_{\{\{p_j\}\}} \prod_{j=1}^{N_s} \prod_{\alpha=1}^{n_j} \chi_{p_j(\alpha)j} (b_j^\dagger)^{n_j} |0\rangle. \quad (42)$$

The sum runs over $\{n\} = (n_1, n_2, \dots, n_{N_s})$, the configurations of occupation numbers with the constraint $\sum_i n_i = N$, and over $\{p_j\}$ with $\sum_{\{\{p_j\}\}} = \sum_{\{p_1\}} \sum_{\{p_2\} \neq \{p_1\}} \sum_{\{p_3\} \neq \{p_1\}, \{p_2\}} \dots$ where $p_j(\alpha)$ is the particle label which takes n_j integer values among N values. The reduced density matrix for a single site is found to be

$$\rho_n = \frac{n!}{\text{Per}(\Omega)} \sum_{n_2, \dots, n_{N_s}} \prod_{i=2}^{N_s} n_i! \left| \sum_{\{\{p_j\}\}} \prod_{j=1}^{N_s} \prod_{\alpha=1}^{n_j} \chi_{p_j(\alpha)j} \right|^2 \quad (43)$$

The explicit expressions of the reduced density matrix for $N = 2$ and $N = 4$ are given in Appendix B. In what follows we will consider the simple case of $N = 4$ bosons. In Fig. 5 we show the probability distribution of the single site entanglement entropy, which, in the absence of disorder, is peaked around $S \simeq 0.62$, broadens under the action of disorder and finally, when disorder becomes strong, develops again a peak but at $S = 0$. We observe that the probability of having zero entropy becomes non-zero only above a disorder threshold that occurs approximately when also the stiffness vanishes, as one can see from Fig. 6.

We have found that in our finite size simulation the crossover between the two limiting behaviors, $P(S)$ peaked either at $S \neq 0$, deep in the superfluid, or close to $S = 0$, deep in the Bose glass, is continuous. We have also noticed that the point at which $P(S)$ becomes finite at $S \simeq 0$ seems to coincide with the point where the stiffness becomes very small, which could be taken as the finite size signal of the superfluid-to-Bose glass transition. This suggests that the behavior of $P(S = 0)$ could be used as well to identify the superfluid-to-Bose glass transition in alternative to the superfluid stiffness in any finite-size numerical simulations. Moreover, we note, looking at Fig. 5, that, close to the transition ($\Delta \approx 4$), the profile of the distribution (the green curve) is almost an equally weighted bimodal, peaked either at small S (insulating regions) and at

$$S \approx S_{SF}(\nu_{eff})$$

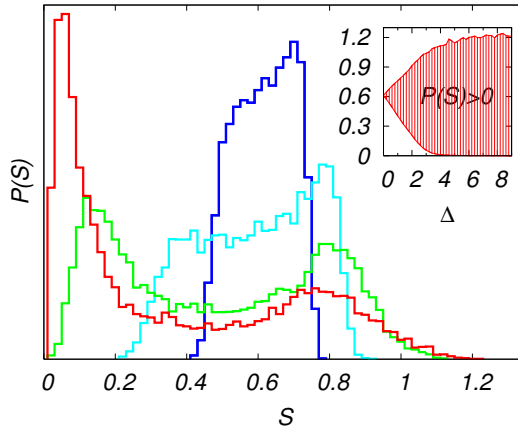


FIG. 5: (Color online) Probability distribution of entropy for $U = 10$ and for different values of disorder strength ($\Delta = 1, 2, 4, 6$). The plot has been made after 10^4 realizations of disorder in a system of $N = 4$ bosons on a 4×4 square lattice. In the inset: the fluctuations of S increase with the strength of disorder and saturate to the maximum value of entropy for 4 bosons which is $\simeq 1.4$

(superfluid regions) given by Eq. (41) where ν is replaced by $\nu_{eff} = \nu/p_c$. The numerical result for the second peak close to the transition ($S \approx 0.8$, for $\nu = 1/4$), is consistent with $p_c \approx 0.59$ which is the site percolation threshold for a square lattice. We have checked this result also with other filling fractions. This finding is in a nice agreement with the percolating droplets scenario.

VI. CONCLUSIONS

We have considered a two-dimensional Bose-Hubbard Hamiltonian in the presence of disorder, and constructed a trial many-body wavefunction by solving a single-particle problem for each boson at a time that feels the effect of all the others as an effective potential. By this wavefunction we have studied the transition between the superfluid and the Bose glass. Beside the vanishing stiffness, we find that the transition can be characterized by the eigenvalues of the matrix of the overlaps between the single-particle wavefunctions. Another quantity we propose to look at is the single-site entanglement entropy. In particular, we argue that when the probability to measure zero entropy becomes finite, $P(S = 0) > 0$, the superfluid start to vanish and the Bose glass phase sets in. The bimodal entropy distribution is, then, the signature of lack of percolation among superfluid clusters.

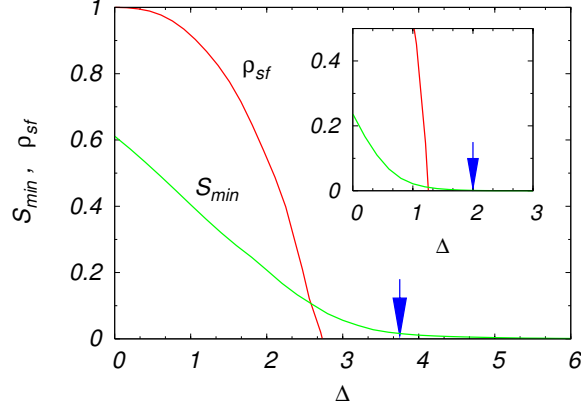


FIG. 6: (Color online) The minimum site entanglement entropy S_{min} (light-green lines) compared with the superfluid stiffness ρ_{sf} (dark-red lines) as functions of the disorder, for $U = 10$ and for filling fraction $\nu = 1/4$ (main plot) and $\nu = 1/16$ (inset). The stiffness, ρ_{sf} , is taken as an average among 400 configurations of disorder for a system of $N = 9$ bosons on a square lattice of 6×6 ($\nu = 1/4$, main plot) and 12×12 ($\nu = 1/16$, inset). The minimum entropy S_{min} is obtained taking the minimum values of S among 10^4 configurations of disorder, and for $N = 4$ on a 4×4 ($\nu = 1/4$, main plot) and 8×8 ($\nu = 1/16$, inset) lattices. The blue arrows point at the transitions, obtained from the overlap matrix method as explained in Sec. II.

Appendix A: Derivation of the action

Let us consider the following wavefunction

$$|\Psi\rangle = \prod_{\alpha} \left(\sum_i \psi_{\alpha i} b_i^{\dagger} \right)^{n_{\alpha}} |0\rangle, \quad (\text{A1})$$

which generalizes Eq. (1) where the integers n_{α} are all equal to 1. Let us define also the overlap matrix $\Omega_{\alpha\beta} = \sum_i \psi_{\alpha i} \psi_{\beta i}^*$ which is Hermitian and positive defined, such that can be parametrized as $\Omega = \psi \psi^{\dagger} = V^{\dagger} |\lambda|^2 V$, in terms of a unitary matrix V . Let us suppose now that another unitary matrix U exists so that we can write $\psi = V^{\dagger} \lambda U$, and define the following bosonic operators

$$b_a^{\dagger} = \sum_i U_{ai} b_i^{\dagger} \quad (\text{A2})$$

$$b_{\alpha}^{\dagger} = \sum_a V_{\alpha a}^{\dagger} b_a^{\dagger}. \quad (\text{A3})$$

Defining also

$$e^{\mathcal{T}} \equiv e^{\sum_a b_a^{\dagger} b_a \ln \lambda_a} \quad (\text{A4})$$

one can then verify that

$$\sum_i \psi_{\alpha i} b_i^\dagger = \sum_a V_{\alpha a}^\dagger \lambda_a b_a^\dagger = e^\mathcal{T} b_\alpha^\dagger e^{-\mathcal{T}} \quad (\text{A5})$$

where we have used the Hausdorff relation

$$\lambda_a b_a^\dagger = e^\mathcal{T} b_a^\dagger e^{-\mathcal{T}}. \quad (\text{A6})$$

Therefore Eq. (A1) can be written as follows

$$|\Psi\rangle = e^\mathcal{T} \prod_\alpha (b_\alpha^\dagger)^{n_\alpha} |0\rangle \quad (\text{A7})$$

Moreover, one can check that

$$e^{\mathcal{T}^\dagger} e^\mathcal{T} = e^{\sum_a b_a^\dagger b_a \ln |\lambda_a|^2} = \frac{1}{\pi} \int \prod_a dz_a dz_a^* e^{-\sum_a |z_a|^2} e^{\sum_a z_a v_a^* b_a^\dagger} e^{\sum_a z_a^* v_a b_a} \quad (\text{A8})$$

with $|\lambda_a|^2 = 1 + |v_a|^2$. Now, in order to rewrite Eq. (A8) on the basis of b_α instead of b_a , we have to define $\hat{v}_{\alpha i} = \sum_a V_{\alpha a}^\dagger v_a U_{ai}$ and $\xi_\alpha = \sum_{i,a} \hat{v}_{\alpha i} U_{ia}^\dagger z_a^*$, and noticing that $\hat{v} \hat{v}^\dagger = \Omega - \mathbb{1}$, we finally have

$$\langle \Psi | \Psi \rangle = \int \prod_\alpha \frac{d\xi_\alpha d\xi_\alpha^*}{\pi} e^{-\xi^\dagger (\Omega - \mathbb{1})^{-1} \xi} \langle 0 | \prod_\beta (b_\beta)^{n_\beta} e^{\sum_\alpha \xi_\alpha^* b_\alpha^\dagger} e^{\sum_\alpha \xi_\alpha b_\alpha} \prod_\gamma (b_\gamma^\dagger)^{n_\gamma} | 0 \rangle \quad (\text{A9})$$

Expanding the exponents and using the commutation relations, in particular the equality $b^m b^{\dagger n} |0\rangle = \frac{n!}{(n-m)!} b^{\dagger(n-m)} |0\rangle$ for $m \leq n$, one can verify that

$$\langle 0 | \prod_\beta (b_\beta)^{n_\beta} e^{\sum_\alpha \xi_\alpha^* b_\alpha^\dagger} e^{\sum_\alpha \xi_\alpha b_\alpha} \prod_\gamma (b_\gamma^\dagger)^{n_\gamma} | 0 \rangle = \prod_\alpha \sum_{m=0}^{n_\alpha} \frac{(n_\alpha!)^2}{(m!)^2 (n_\alpha - m)!} |\xi_\alpha|^{2m} \quad (\text{A10})$$

equal to $\prod_\alpha n_\alpha! L_{n_\alpha}^0(-|\xi_\alpha|^2)$, using the definition of the generalized Laguerre polynomials, $L_n^k(z) = \sum_{m=0}^n \frac{(n+k)!}{m!(k+m)!(n-m)!} (-z)^m$, which can be written also in terms of confluent hypergeometric functions, $L_n^k(z) = \frac{(k+n)!}{k!n!} {}_1F_1(-n, k+1; z)$. As a final result the norm of (A1) can be written as an integral, Eq. (2), with the action

$$\mathcal{S}(\xi, \xi^\dagger) = \xi^\dagger (\Omega - \mathbb{1})^{-1} \xi - \sum_\alpha \ln \left[n_\alpha! L_{n_\alpha}^0(-|\xi_\alpha|^2) \right]. \quad (\text{A11})$$

If $n_\alpha = 1, \forall \alpha$, since $L_1^0(-|\xi_\alpha|^2) = (1 + |\xi_\alpha|^2)$, the action reduces to Eq. (3). The saddle point equation reads then

$$\xi_\alpha = \sum_{\beta, n_\beta > 0} (\Omega_{\alpha\beta} - \delta_{\alpha\beta}) \frac{L_{(n_\beta-1)}^1(-|\xi_\beta|^2)}{L_{n_\beta}^0(-|\xi_\beta|^2)} \xi_\beta, \quad (\text{A12})$$

which reduces to Eq. (4), for all $n_\alpha = 1$. Since, for $|\xi_\beta|^2 \ll 1$, we can expand $L_n^k(-|\xi_\beta|^2) \simeq \frac{(n+k)!}{n!k!} \left(1 + \frac{n}{k+1} |\xi_\beta|^2\right)$, the eigenvalue equation, when discarding $O(\xi_\beta^3)$ terms in the r.h.s. of Eq. (A12), becomes

$$\xi_\alpha = \sum_{\beta} (\Omega_{\alpha\beta} - \delta_{\alpha\beta}) n_\beta \xi_\beta, \quad (\text{A13})$$

which generalizes Eq. (5) for arbitrary n_β .

Appendix B: Reduced density matrix: two simple cases

Here we are going to show within a toy model made of 2 bosons arranged on 3 sites how disorder and interaction can conspire to enhance the bipartite entanglement entropy. With two bosons $N = 2$ and without disorder, in the delocalized phase, $|\zeta_1|^2 = 1/3$, from Eqs. (38), (33), we get the following single site entropy

$$S = 2 \ln 3 - \frac{16}{9} \ln 2 \simeq 0.96 \quad (\text{B1})$$

What we shall be seeing in the following is that this value can be overcome introducing a suitable amount of disorder.

If we now take Eq.(42) as the many body wave function, we get, for $N = 2$ bosons and generic N_s sites, the following three diagonal elements of the reduced density matrix

$$\rho_0 = \frac{1}{\text{Per}(\Omega)} \sum_{i=2}^{N_s} \left(2|\chi_{1i}\chi_{2i}|^2 + \sum_{j>i}^{N_s} |\chi_{1i}\chi_{2j} + \chi_{2i}\chi_{1j}|^2 \right) \quad (\text{B2})$$

$$\rho_1 = \frac{1}{\text{Per}(\Omega)} \sum_{i=2}^{N_s} |\chi_{11}\chi_{2i} + \chi_{21}\chi_{1i}|^2 \quad (\text{B3})$$

$$\rho_2 = \frac{2}{\text{Per}(\Omega)} |\chi_{11}\chi_{21}|^2 \quad (\text{B4})$$

Let us now consider $N_s = 3$ and a simple on site disorder such that $\epsilon_i = \pm\Delta$. We can have therefore 8 possible configurations of disorder. For $U \gg \Delta$, by semiclassical considerations and using Eqs. (B2-B4), we can have probability $\sim 1/4$ to have $S \simeq 0$, i.e. $P(S \simeq 0) \simeq 1/4$ while $P(S \simeq \ln 2) \simeq 1/2$ and $P(S \simeq 0.96) \simeq 1/4$, the same entropy as without disorder. For $U \ll \Delta$, instead, we have $P(S \simeq 0) \simeq 1/2$, $P(S \simeq 0.96) \simeq 1/4$ and $P(S \simeq \frac{3}{2} \ln 2 \simeq 1.04) \simeq 1/4$, namely we can have a sizable probability to have maximum entropy for two bosons, so to exceed the value in Eq. (B1). The disorder, therefore, peaks the probability distribution at zero while widening the entropy fluctuations.

In general for filling $\nu < 1$, the superfluid single site entropy is $S \simeq \nu(1 - \ln \nu)$, as shown in the text. By introducing strong enough disorder there is the possibility for a fraction k of the total sites to have very large local energies which make those sites inaccessible for the particles. This induces a larger effective filling, $\frac{\nu}{1-k}$, and consequently enhances the entropy.

For the sake of completeness we hereafter report the form of the reduced density matrix for $N = 4$ bosons, used in the paper in Sec. V B. To simplify notation we define the matrix

$$\mathcal{L}^{ijkl} = \begin{pmatrix} \chi_{1i} & \chi_{1j} & \chi_{1k} & \chi_{1l} \\ \chi_{2i} & \chi_{2j} & \chi_{2k} & \chi_{2l} \\ \chi_{3i} & \chi_{3j} & \chi_{3k} & \chi_{3l} \\ \chi_{4i} & \chi_{4j} & \chi_{4k} & \chi_{4l} \end{pmatrix} \quad (\text{B5})$$

so that the single site reduced density matrix can be written in the following form:

$$\rho_0 = \frac{1}{\text{Per}(\Omega)} \sum_{i=2}^{N_s} \left\{ \sum_{j>i}^{N_s} \sum_{k>j}^{N_s} \sum_{l>k}^{N_s} |\text{Per}(\mathcal{L}^{ijkl})|^2 + \frac{1}{2!} \sum_{j \neq i}^{N_s} \sum_{k \neq i,j}^{N_s} |\text{Per}(\mathcal{L}^{iijk})|^2 \right. \quad (\text{B6})$$

$$\left. + \frac{1}{2!2!} \sum_{j>i}^{N_s} |\text{Per}(\mathcal{L}^{iijj})|^2 + \frac{1}{3!} \sum_{j \neq i}^{N_s} |\text{Per}(\mathcal{L}^{iiij})|^2 + \frac{1}{4!} |\text{Per}(\mathcal{L}^{iiii})|^2 \right\}$$

$$\rho_1 = \frac{1}{\text{Per}(\Omega)} \sum_{i=2}^{N_s} \left\{ \sum_{j>i}^{N_s} \sum_{k>j}^{N_s} |\text{Per}(\mathcal{L}^{1ijk})|^2 + \frac{1}{2!} \sum_{j \neq i}^{N_s} |\text{Per}(\mathcal{L}^{1iij})|^2 + \frac{1}{3!} |\text{Per}(\mathcal{L}^{1iii})|^2 \right\} \quad (\text{B7})$$

$$\rho_2 = \frac{1}{\text{Per}(\Omega)} \sum_{i=2}^{N_s} \left\{ \frac{1}{2!} \sum_{j>i}^{N_s} |\text{Per}(\mathcal{L}^{11ij})|^2 + \frac{1}{2!2!} |\text{Per}(\mathcal{L}^{11ii})|^2 \right\} \quad (\text{B8})$$

$$\rho_3 = \frac{1}{\text{Per}(\Omega)} \frac{1}{3!} \sum_{i=2}^{N_s} |\text{Per}(\mathcal{L}^{111i})|^2 \quad (\text{B9})$$

$$\rho_4 = \frac{1}{\text{Per}(\Omega)} \frac{1}{4!} |\text{Per}(\mathcal{L}^{1111})|^2 \quad (\text{B10})$$

From equations above one can easily guess the form of the reduced density matrix for a generic value of N .

[1] D. Jaksch, C. Bruder, J. I. Cirac, C. W. Gardiner, and P. Zoller, Phys. Rev. Lett. **81**, 3108 (1998).

- [2] I. Bloch, J. Dalibard, and W. Zwerger, *Rev. Mod. Phys.* **80**, 885 (2008).
- [3] J. Billy, V. Josse, Z. Zuo, A. Bernard, B. Hambrecht, P. Lugan, D. Clement, L. Sanchez-Palencia, P. Bouyer, and A. Aspect, *Nature* **453**, 891 (2008).
- [4] G. Roati, C. D’Errico, L. Fallani, M. Fattori, C. Fort, M. Zaccanti, G. Modugno, M. Modugno, and M. Inguscio, *Nature* **453**, 895 (2008).
- [5] L. Fallani, J. E. Lye, V. Guarrera, C. Fort, and M. Inguscio, *Phys. Rev. Lett.* **98**, 130404 (2007).
- [6] C. Chin, R. Grimm, P. Julienne, and E. Tiesinga, *Rev. Mod. Phys.* **82**, 1225 (2010).
- [7] S. Rapsch, U. Schollowck, and W. Zwerger, *EPL (Europhysics Letters)* **46**, 559 (1999).
- [8] J.-W. Lee, M.-C. Cha, and D. Kim, *Phys. Rev. Lett.* **87**, 247006 (2001).
- [9] B. Damski, J. Zakrzewski, L. Santos, P. Zoller, and M. Lewenstein, *Phys. Rev. Lett.* **91**, 080403 (2003).
- [10] N. Prokof’ev and B. Svistunov, *Phys. Rev. Lett.* **92**, 015703 (2004).
- [11] P. Buonsante, F. Massel, V. Penna, A. Vezzani, *Laser Physics* **18**, 653 (2008).
- [12] U. Bissbort, R. Thomale, and W. Hofstetter, *Phys. Rev. A* **81**, 063643 (2010).
- [13] L. Pollet, N. V. Prokof’ev, B. V. Svistunov, and M. Troyer, *Phys. Rev. Lett.* **103**, 140402 (2009).
- [14] V. Gurarie, L. Pollet, N. V. Prokof’ev, B. V. Svistunov, and M. Troyer, *Phys. Rev. B* **80**, 214519 (2009).
- [15] J. Carrasquilla, F. Becca, A. Trombettoni, and M. Fabrizio, *Phys. Rev. B* **81**, 195129 (2010).
- [16] T. Giamarchi and H. J. Schulz, *EPL (Europhysics Letters)* **3**, 1287 (1987).
- [17] T. Giamarchi and H. J. Schulz, *Phys. Rev. B* **37**, 325 (1988).
- [18] M. P. A. Fisher, P. B. Weichman, G. Grinstein, and D. S. Fisher, *Phys. Rev. B* **40**, 546 (1989).
- [19] J. K. Freericks and H. Monien, *Phys. Rev. B* **53**, 2691 (1996).
- [20] W. Krauth, N. Trivedi, and D. Ceperley, *Phys. Rev. Lett.* **67**, 2307 (1991).
- [21] R. V. Pai, R. Pandit, H. R. Krishnamurthy, and S. Ramasesha, *Phys. Rev. Lett.* **76**, 2937 (1996).
- [22] P. Buonsante and A. Vezzani, *Phys. Rev. Lett.* **98**, 110601 (2007).
- [23] L. Amico, R. Fazio, A. Osterloh, and V. Vedral, *Rev. Mod. Phys.* **80**, 517 (2008).
- [24] M. Haque, O. S. Zozulya, and K. Schoutens, *J. Phys. A: Math. Theor.* **42**, 504012 (2009).
- [25] H. Katsura, N. Kawashima, A. N. Kirillov, V. E. Korepin, S. Tanaka, *J. Phys. A: Math.*

Theor. **43** 255303 (2010).

- [26] P. W. Anderson, *Basic notions of condensed matter physics* (Benjamin, Manlo Park CA, 1984).